BBA - Molecular Basis of Disease 1865 (2019) 1160–1169

Contents lists available at ScienceDirect

BBA - Molecular Basis of Disease

journal homepage: www.elsevier.com/locate/bbadis

# Tissue plasminogen activator and neuropathy open the blood-nerve barrier with upregulation of microRNA-155-5p in male rats

Ann-Kristin Reinhold[a], Shaobing Yang[a,c], Jeremy Tsung-Chieh Chen[a], Liu Hu[a,c], Reine-Solange Sauer[a], Susanne M. Krug[b], Egle M. Mambretti[a], Michael Fromm[b], Alexander Brack[a], Heike L. Rittner[a,*]

[a] Dept. of Anesthesiology, University Hospital of Würzburg, 97080 Würzburg, Germany
[b] Institute of Clinical Physiology, Charité – Universitätsmedizin Berlin, Campus Benjamin Franklin, 12200 Berlin, Germany
[c] Dept. of Anesthesiology and Pain Medicine, Tongji Hospital of Tongji Medical College, Huazhong University of Science and Technology, 430030 Wuhan, China

ARTICLE INFO

*Keywords:*
(4–6): Chronic constriction injury
microRNA
Tight junction
Adherens junction
Neuropathic pain
Blood nerve barrier

ABSTRACT

The blood-nerve barrier (BNB) consisting of the perineurium and endoneurial vessels is sealed by tight junction proteins. BNB alterations are a crucial factor in the pathogenesis of peripheral neuropathies. However, barrier opening, e.g. by tissue plasminogen activator (tPA), can also facilitate topical application of analgesics. Here, we examined tPA both in the pathophysiology of neuropathy-induced BNB opening or via exogenous application and its effect on the cytoplasmatic tight junction protein anchoring protein, zona occludens-1 (ZO-1), the adherens molecule JAM-C and microRNA(miR)-155-5p. Specifically, we investigated whether tPA alone and barrier opening lead to pain behavioral changes, i.e. hyperalgesia, or whether these effects require further factors.

Male Wistar rats underwent chronic constriction injury (CCI) or were treated by a single perisciatic application of recombinant (r)tPA. CCI elicited mechanical allodynia, tPA mRNA upregulation, macrophage invasion, BNB leakage for large molecule tracers, downregulation of ZO-1 and JAM-C mRNA/protein, and a loss of immunoreactivity of both in perineurium and endoneurial cells. Similarly, after perisciatic rtPA injection, ZO-1 and JAM-C mRNA as well as cytosolic/membrane protein and ZO-1 immunoreactivity were downregulated, and the BNB was opened. Neither mechanical hypersensitivity nor macrophage infiltration was observed after rtPA in contrast to CCI. Mechanistically, miR-155-5p, which is known to destabilize barriers and tight junction proteins like claudin-1 and ZO-1, was increased in CCI and to lesser extent after rtPA application. In summary, tPA transiently opens the BNB possibly via miR-155-5p. However, tPA does not provoke allodynia in the absence of a neuropathic stimulus like a ligation or inflammation.

## 1. Introduction

Neuropathic pain is defined as pain caused by a lesion or disease of the somatosensory nervous system. It can arise from several etiologies. With a prevalence of 7–10% [43], it is not only wearing on the patients affected but constitutes also significant socioeconomic burden. Moreover, as classical analgesic agents such as opioids are not very effective, treatment still proves difficult necessitating the identification of new targets [10].

A number of peripheral molecular mechanisms have been identified that contribute to neuropathy, e.g. inflammatory or regenerational pathways. TPA has been recognized as one such factor. tPA causes fibrinolytic activity after CCI, thereby facilitating functional recovery of the affected nerve [49,53]. On the other hand, tPA is associated with increased neuronal excitability and mechanical hypersensitivity after peripheral nerve injury or when given intrathecally [4,45]. RtPA is widely used for lysis therapy in thromboembolic stroke. In addition, rtPA increases blood brain barrier (BBB) permeability via downregulation of the tight junction protein claudin-5, occludin and intracellular scaffolding protein ZO-1 due to increased matrix metalloproteinases (MMP)-9 activity [25]. Recently, we could show that in the peripheral nerve, rtPA downregulates tight junction proteins in the BNB

*Abbreviations:* BBB, blood-brain barrier; BNB, blood-nerve barrier; CCI, chronic constriction injury; EBA, Evans blue albumin; JAM, junctional adhesion molecules; LRP-1, low density lipoprotein receptor-related protein 1; MMP, metalloproteinase; rtPA, recombinant tissue plasminogen activator; ZO-1, zonula occludens protein 1

* Corresponding author at: Dept. Anesthesiology and Critical Care, University of Würzburg, Oberduerrbacher Strasse 6, D-97080 Würzburg, Germany.
*E-mail address:* rittner_h@ukw.de (H.L. Rittner).

https://doi.org/10.1016/j.bbadis.2019.01.008
Received 5 July 2018; Received in revised form 30 November 2018; Accepted 4 January 2019
Available online 06 January 2019
0925-4439/ 

via binding to Low Density Lipoprotein Receptor-related Protein 1 (LRP-1) and ERK phosphorylation [47].

The BNB consists of the perineurium surrounding nerve fascicles and the endothelium of endoneurial blood vessels [32]. Perineurial cells or endoneurial cells are connected by adherens junctions and sealed by tight junctions. In the perineurium, we and others have already shown expression of occludin, claudin-1, claudin-3, claudin-19, tricellulin and ZO-1 [13,20,26,36]. ZO-1 is required for the organization of the integral membrane proteins linking junctional molecules such as claudin and occludin to the actin cytoskeleton via its PDZ domain. It is thus crucial for tight junctions sealing: In ZO-1 knockout mice, yolk sac defects lead to embryonic lethality at around E11.5 [16]. Cadherins and catenin as well as junctional adhesion molecules (JAMs) form adherens junctions. The family of JAMs comprises JAM-A, −B, and −C and belongs to the immunoglobulin superfamily. Through its intracellular C-terminal type II PDZ binding motif, JAMs interact with scaffolding molecules such as ZO-1 and the actin skeleton [8,15]. JAM-C has been primarily identified in vascular and epithelial cells. In the peripheral nerve, it is found in junctional regions of Schwann cells [37] and is crucial for the integrity of myelinated peripheral neurons. In peripheral neuropathy, the BNB is unsealed with a reduction in the scaffolding protein ZO-1 [20] allowing for the invasion of leukocytes and the diffusion of potentially neurotoxic mediators like cytokines to elicit pain. After sciatic crush injury, Avari et al. showed downregulation of JAM-C, followed by recuperation in the further course, correlating with remyelination of neurons [3].

MiRs are small, ~20 nt long non-coding single-stranded RNAs. Mature miRNAs form imperfect homology with the 3′UTR in a target mRNA, thereby preventing translation or promoting mRNA degradation. MiR-29b is a regulator of claudin-1 in the intestinal barrier [51], and miR-125 of the BBB [31]. Also miR-155 is known to affect barriers: overexpression in endothelial cells inhibits endothelial cell proliferation and migration. Both in vivo and in vitro, it increases vascular endothelial permeability via re-endothelialization [50]. Another recent study on the BBB showed the effect of miR-155 on endothelial tight junctions after oxygen-glucose deprivation (OGD). MiR-155 inhibitors attenuate the effect of OGD, i.e. result in an increase of not only the direct target claudin-1, but also ZO-1. Moreover, interaction between these two tight junction proteins is strengthened, leading to endothelial membrane stabilization [29]. Moreover, the miR destabilizes BBB function in neuroinflammation: Lopez-Ramirez et al. showed a strong upregulation of miR-155-5p at the neurovascular unit in human multiple sclerosis and its rodent equivalent autoimmune encephalomyelitis, leading to junctional disorganization and increased permeability by targeting claudin-1 [22]. [29].

In the peripheral nerve, tPA binds to LRP-1 [47]. LRP-1 agonists are also known to induce miR-155-5p [23]. Thus, an effect of tPA on the BNB by increasing permeability via miR-155 induction is conceivable. This study was therefore designed to explore the role of (r)tPA in peripheral neuropathy and after perineural administration, notably its effect on BNB homeostasis with respect to scaffolding protein ZO-1 and JAM-C as well as on miR-155-5p. To this end, two conditions, CCI and perineural rtPA injection, were compared.

## 2. Materials and methods

### 2.1. Animals, models and treatment schedules

Animal protocols were approved by the animal care committee of the provincial government of Würzburg. Male Wistar rats (Janvier labs, Le Genest-St-Isle, France) weighing 180–250 g, free of pathogenic microorganisms, were housed in groups of six in cages in a circadian light rhythm (12 h:12 h light/dark cycle, 21–25 °C, 45–55% humidity) with food and water ad libitum as well as enrichment tools. Animals were randomly assigned to treatments so that treated and control animals were in different number in one cage. Experiments were conducted during daytime and at indicated time points. Handling procedures were in accordance with international guidelines for the care and use of laboratory animals (EU Directive 2010/63/EU for animal experiments) and the guidelines of the IASP [14]. Score sheets with defined end points were used daily for animal well-being.

Three experimental groups were compared in neuropathy experiments at different time points: CCI, sham and naïve (control) rats. CCI was accomplished by exposing the sciatic nerve at the right mid-thigh and placing four loose silk ligatures (4/0 Permasilk, Ethicon Inc., Somerville, NJ, USA) with about 1-mm spacing around the nerve under deep isoflurane anesthesia (maintenance with 2 Vol%, $FiO_2$ 1.0). Absence of paw withdrawal indicated adequate surgical anesthesia. Great care was taken to avoid harming the nerve with surgical tools. The wound was closed with sutures (Prolene 3.0, Ethicon Inc., Somerville, NJ, USA). In sham-operated rats, the sciatic nerve was briefly exposed without introducing or performing ligatures. [18,35].

For BNB opening, rtPA was applied perineurally. Two experimental groups were compared: rtPA and solvent-treated control rats. Under brief isoflurane anesthesia (2 Vol%, $FiO_2$ 1.0), the right sciatic nerve was located using a 22 G atraumatic needle (to avoid intraneural injection) connected to a nerve stimulator (Stimuplex Dig RC; Braun, Melsungen, Germany) as previously described [54]. The needle was initially placed according to anatomical landmarks. Perisciatic location was verified by persistent twitching of the lower leg under reduction of the current. Rats received either a perisciatic injection of 150 µl 0.9% NaCl or 10 µg rtPA (Actilyse; Boehringer Ingelheim, Biberach, Germany) in 150 µl 0.9% saline. Both solution were freshly prepared from sterile flasks to prevent accidental contamination. At indicated time points, reflexive pain behavior tests were performed before and after treatment. Tissue samples were taken as outlined. Inhalational isoflurane was chosen for its fast and versatile controllability.

Experimental groups with CCI/sham/naïve included 6 animals/group and with rtPA/saline injection 8 rats/groups based on an a priori power analysis (G Power 3.1, gpower.hhu.de, [9]) (effect size 1.67, $p < 0.05$, *t*-test). In few experiments (mRNA quantification after tPA), the n-number is lower due to accidental sample loss during tissue extraction. For qualitative data in immunohistochemistry and BNB permeability, three animals/group were analyzed. Primary endpoints in different cohorts were change in pain behavior, altered tight junction of adherens junction mRNA or protein expression and altered miR expression.

### 2.2. Measurement of BNB permeability

To evaluate the permeability, harvested sciatic nerves were immediately fixed with 1% paraformaldehyde for 1 h and immersed in 2 ml of Evans blue albumin (EBA, 5% bovine albumin labeled with 1% Evans blue; both from Sigma Chemicals) for 1 h. Afterwards, tissue was embedded in TissueTek O.C.T. compound (Sakura, Finetek Europe B.V., AV Alphen aan den Rijn, Netherlands), 10 µm sections obtained and analyzed by confocal microscopy (Zeiss LSM 710 and 510 META, Jena, Germany). Semiquantification of endoneurial fluorescence intensities was performed using ImageJ 1.51. To define the endoneurial region of interest (ROI), the endoneurial/perineurial border of each nerve was defined using the brightfield setting and transferred to the fluorescence image. Pixel values were measured and integrated over the area [33].

### 2.3. Western blotting

Sciatic nerve tissue close to the site of injury (CCI) or in the area of rtPA application was harvested. Per sample, nerves of two rats were pooled. Samples were homogenized in lysis buffer for Triton X-100 soluble proteins (25 mM Tris pH 7.6, 120 mM NaCl, 2 mM ethylenediaminetetraacetic acid (EDTA), 25 mM NaF, 1% (v/v) Triton X 100) containing protease inhibitors (Complete, Roche Applied Science) [54]. Triton X-100, a non-ionic detergent, permeabilizes cell membranes and

is often used in lysis buffers. In this study, we compared the Triton-X-100 soluble fraction, presumed to contain mainly cytosolic proteins, and an insoluble fraction, inferred to contain cell membrane proteins as described before [34,41]. Triton-X-100 soluble ("cytosol") fractions were obtained by homogenization with minipistil and sonification (3 × 5 s/3 s break), followed by a centrifugation at 4500 ×*g* for 10 min and subsequent centrifugation of the remaining supernatant at 40,000 ×*g* for 30 min. The Triton X-100-insoluble pellet ("membrane fraction"), was resuspended in an equal volume of extraction buffer (25 mM Hepes pH 7.6, 2 mM EDTA, 25 mM NaF, 1% (w/v) sodium dodecyl sulfate (SDS)). Extracted protein was diluted in lysis buffer and incubated with BCA protein assay reagent (Pierce, Rockford, IL, USA) for quantification on a plate reader (Tecan, Grödig, Austria). Aliquots of protein were mixed with SDS containing buffer (Laemmli buffer), denatured at 95 °C for 5 min, fractionated on SDS polyacrylamide gels and subsequently blotted onto PVDF membranes (PerkinElmer, Boston, MA, USA). Proteins were detected using specific antibodies: rabbit polyclonal anti-ZO-1 (1:200; 1A12, Thermo Fisher Scientific, Waltham, MA, USA), rabbit polyclonal anti-JAM-C (1: 500; ABT31, Merck Millipore, Darmstadt, Germany) and as protein loading control β-actin (mouse anti-β-actin 1: 20,000; A3854, Sigma Aldrich, St. Louis, MO, USA). Peroxidase-conjugated goat anti-rabbit IgG, goat anti-mouse IgG and the chemiluminescence detection system Lumi-Light PLUS Western blotting kit (Roche, Mannheim, Germany) were used to detect bound antibodies. Quantification was done by densitometry (Alpha Innotech, Santa Clara, CA, USA; FluorChem FC2 Imaging systems, Multilmage II): The density of the spots was quantified as integrated density value (IDV) per area (IDV = mean grey value of ROI x area of ROI).

### 2.4. Immunofluorescence and confocal microscopy

Under very deep isoflurane anesthesia (4 Vol%, $FiO_2$ 1.0), rats were perfused with 4% paraformaldehyde (PFA). Sciatic nerves were removed and post-fixed in 4% PFA for about 120 min and were cryoprotected overnight at 4 °C in 10% sucrose. The nerves were embedded in Tissue Tek O.C.T. Compound and were frozen in liquid nitrogen.

Frozen sciatic nerve tissue was cut in sections and fixed with icecold (−20 °C) ethanol. Sections were prepared from nerve tissue proximal to the site of injury (CCI) or within the area of rtPA application. Tissue sections were permeabilised with 0.5% Triton-X100 (in phosphate-buffered saline) and blocked in 2% goat serum in phosphate-buffered saline. In a next step, they were incubated with primary antibodies rabbit anti-JAM-C (1:500; ABT31, Merck Millipore, Darmstadt, Germany) and monoclonal mouse anti-ZO-1 (1:200; 1A12, Invitrogen/Thermo Fisher Scientific, Waltham/MA, USA) overnight, following sequential incubation with secondary antibodies: goat anti-rabbit IgG Alexa Fluor 594 (1:500; A21207, Invitrogen/Thermo Fisher Scientific, Waltham/MA, USA), and/or goat anti-rabbit Alexa Fluor 488 or 647 (1:500; Life Technologies/Thermo Fischer). DAPI (Roche, Mannheim, Germany) was used to stain the nuclei. ProTag Mount-Fluor was employed for mounting the sections (Biocyc, Luckenwalde, Germany), and confocal laser-scanning microscopy was performed (Zeiss LSM 710 and 510 META, Jena, Germany).

Quantification of staining signal intensities was performed using ImageJ 1.50 g. The inner perineurium was used as ROI and pixel values were measured and integrated over the area.

### 2.5. PCR

Sciatic nerve tissue (site of the ligation in CCI or area of rtPA injection) was dissected. Total RNA was extracted with Trizol (Invitrogen) and 1 μg was transcribed to cDNA using the high capacity cDNA-kit (Applied Biosystems, Life technologies) following manufacturer's instructions. GAPDH was used as a reference gene for quantification. qPCR analysis was performed with the following custom-made primers (MWG Eurofins, Ebersberg, Germany) using the SYBRGreen method: tPA (fw TCAGATGAGATGACAGGGAAATGCC, and rev ATCA TACAGTTCTCCCAGCC); ZO-1 (fw CACGATGCTCAGAGACGAAGG, and rev TTCTACATATGGAAGTTGGGGATC); JAM-C (fw TGCTGCTCTTCA GGGGCTGCGTGAT, and rev AACACATCTGTGCGACCGGCCAGGT), GAPDH (fw AGTCTACTGGCGTCTTCAC, and rev TCATATTTCTCGTG GTTCAC). A prior melt-curve analysis did not reveal formation of primer-dimers or several products. qPCR analysis was carried out by a 7300 Real-Time PCR System (Applied Biosystems, Thermo Fischer) with the following program: 95 °C for 10 min, and 40 cycles at 95 °C for 15 s and 60 °C for 1 min. Samples were analyzed as triplicates. Relative mRNA abundances to GAPDH were calculated by the ΔΔCt method (threshold cycle value, [21]). To compare different samples, the control condition (untreated animals) was set at 1.

### 2.6. Neurohistology

Sciatic nerves were obtained 7 d after CCI or 7 d after rtPA. The time points were chosen because a certain time interval after nerve damage is necessary for immune cell infiltration and necessary to see possible damage [38,39]. Sections proximal to the site of injury (CCI) or in the area of rtPA application were analyzed. Infiltration of nerves with macrophages was analyzed in 10-μm cryosections using a monoclonal mouse anti-rat antibody to CD68 (ED1, Linaris, Germany). An avidin-biotin complex (Vector Laboratories) was utilized as a secondary system. Staining was visualized with 3,3″-diaminobenzidine tetrahydrochloride (DAB) [47].

### 2.7. Behavioral testing

Before and after CCI or rtPA injection, mechanical allodynia was determined using the von Frey test. A series of von Frey filaments (Aesthesio® set, UGO BASILE) were assessed to record the withdrawal threshold of the hind paw and identify mechanical allodynia response and touch sensitivity after surgery or drug injection. Treatments were randomized and blinded. In general, the filaments were applied to the plantar surface of the hind paw and were held for 1–3 s, until the filaments were bent to an angle of 45°. Each paw received stimuli from different forces of the filament, with a 30-s recovery period between each application. The 50% paw withdrawal threshold of von Frey filaments response was determined using Dixon's up and down method [6].

### 2.8. Quantification of miR expression

For miR expression analysis, 70 ng of total RNA was applied for reverse transcription to synthesize cDNA of miRNA using TaqMan MiR Reverse Transcription Kit (Thermo Fischer). qRT-PCR analysis was performed using TaqMan Universal Master Mix II, No UNG (2×) (Thermo Fischer) and primers designed for miRs (Thermo Fischer): mmu-miR-155-5p (ID 002571) and U6 snRNA (ID 001973). These miR primers had identical sequences in the rat (rno-miR). U6 was used as an endogenous control for normalization. 20 μl of the reverse transcription mix was amplified by PCR with the following program: 95 °C for 10 min, and 40 cycles at 95 °C for 15 s and 60 °C for 1 min. Each sample was analyzed in triplicates. Relative miR abundances to U6 snRNA were calculated by the ΔΔCt method (the threshold cycle value) with the control condition (untreated animals) set at 1.

### 2.9. Statistical analysis

Data are presented as mean ± SEM. Two groups were compared by *t*-test for independent variables. Multiple measurements with one or two variables (e.g. time and treatment) were analyzed by One- or Two-Way ANOVA or by repeated measurements (RM) Two-Way ANOVA, as appropriate, and described in the figure legends. Multiple testing correction was performed using Holm-Sidak post-hoc test. Differences

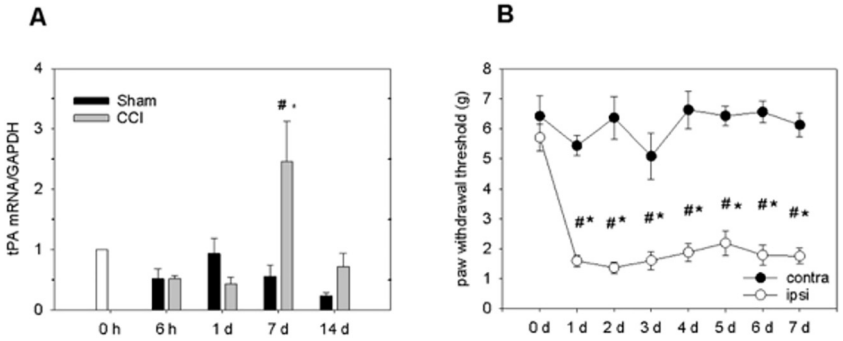


**Fig. 1.** CCI leads to tPA upregulation and allodynia. **A** Wistar rats underwent CCI or sham operation. Ipsilateral sciatic nerves were harvested at indicated time points for up to 14 d, tPA mRNA measured and compared to sham (* $p < 0.05$) or to naïve controls (# $p < 0.05$). n = 5–6, two-way ANOVA, Holm-Sidak post hoc test. **B** Paw withdrawal thresholds (g) to measure mechanical allodynia were obtained using the von Frey method before or after CCI surgery for up 7 d. The ipsilateral (white) and the to the contralateral side (black) were compared (* $p < 0.05$ compared to contralateral side, # $p < 0.05$ compared to baseline value at 0 h). n = 7, two-way RM ANOVA and Holm-Sidak post hoc test. All data is presented as mean ± SEM.

were considered significant if $p < 0.05$.

## 3. Results

### 3.1. Tissue plasminogen activator upregulation and BNB opening after CCI

To explore the role of tPA in the BNB, we first quantified tPA mRNA in the sciatic nerve after CCI. tPA mRNA was increased around 4.4-fold compared to sham-operated animals prominently 7 d after CCI, while we found no changes at earlier time points. Mechanical hypersensitivity measured by von Frey test occurred soon after nerve injury and developed into a full-fledged neuropathic phenotype within 7 d (Fig. 1). No adverse events occurred in the CCI or sham group.

Next, we explored barrier leakiness and expression of tight and adherens junction proteins after CCI. CCI led to an opening of the BNB: 1 d after CCI, EBA (68 kDa) had permeated the BNB, was taken up by the nerve and significantly accumulated in the endoneurium, which was not observed in sham-operated animals ($p < 0.05$) (Fig. 2A, B). In line with this, mRNA of ZO-1 and JAM-C were downregulated in the operated nerve already 6 h after surgery. ZO-1 mRNA was decreased by 52% compared to sham control, a trend that only intensified over the period observed: After 14 d, it was reduced by 84% compared to sham, and 80% compared to naïve animals (Fig. 2C). ZO-1 protein expression developed likewise: After 6 h, expression in the nerve was decreased by 56% compared to sham control and persevered further in the process, with a minimum of 10% of sham expression, or 11% compared to naïve control after 1 d. Notably, in sham-operated animals, an initial decrease compared to naïve controls (at 6 h) was observed which recovered quickly. (Fig. 2D). JAM-C was downregulated in a similar manner: After 6 h, mRNA was reduced by 68% compared to sham-operated animals and by 79% after 14 d (Fig. 2E). On the protein level, expression differed between Triton X-100 soluble (“cytosol”) and insoluble (“membrane”) fractions of the sciatic nerve: In the former, the expression pattern was initially similar to that of ZO-1, with a decrease around 50% after 6 h and 1 d. However, it remained at a rather stable level over the period observed, with a downregulation by 44% after 14 d (Fig. 2F). JAM-C expression in the Triton X-100 insoluble fraction (“membrane”), in contrast, was downregulated significantly only after 1 and 14 d (Fig. 2G).

ZO-1 immunoreactivity was prominent in both perineurium and endoneurium. A similar distribution pattern applied to JAM-C, however, with intense crescent-shape immunoreactivity also found in the endoneurium, presumably Schwann cells surrounding axons within the sciatic nerve. In line with the mRNA and protein results, immunohistochemistry stainings of the nerve 1 d after CCI revealed a lower fluorescence intensity for both proteins (Fig. 3). While ZO-1 immunoreactivity was visibly downregulated in both perineurium and endoneurium (Fig. 3A), JAM-C immunofluorescence decreased mainly in the endoneurium (Fig. 3B). Moreover, the perineurial structure appeared less defined. While preparations from sham-operated animals showed a well-defined dense line of immunoreactivity, it was less intense and fragmented after CCI. This was further confirmed by semiquantification of fluorescence intensity (Fig. 3C): Compared to naïve controls or sham-operated animals, ZO-1 intensity was decreased by 38% and 42%, respectively, after CCI. Similarly, JAM-C intensity was decreased by 45% and 41%, respectively.

### 3.2. Increased permeability of the BNB by rtPA without nerve damage

To elucidate the effect of tPA on BNB permeability and tight/adherens junction protein expression, we applied exogenous rtPA in vivo. A single perisciatic rtPA injection (10 µg) led to a barrier breach within 2 h after application, as shown by the EBA permeability test with increased fluorescence in the endoneurium of the sciatic nerve. This was not observed in sham-operated animals. (Fig. 4A, B). No other clinical adverse events (e.g. bleeding, symptoms of hemorrhagic stroke) were observed after rtPA application, animals roamed around unaltered. As shown by qPCR, mRNA of ZO-1 and JAM-C were both downregulated after 2 h, ZO-1 by 40% (Fig. 4C); JAM-C by 15% (Fig. 4E). A similar pattern emerged on the protein level: Within 1 h after injection, ZO-1 expression in the sciatic nerve decreased by 43%, a robust effect observed for the entire 24 h (Fig. 4D). Interestingly, JAM-C expression differed between Triton X-100 soluble and insoluble (“cytosol” and “membrane”) of the nerve: While expression in the former was decreased by 30–33% over the entire 24 h (Fig. 4F), downregulation in the latter was far stronger, with a reduction by 62% after 1 h and 57% still after 24 h (Fig. 4G).

These observations were endorsed by immunohistochemistry (Fig. 5). Moreover, the perineurial barrier after rtPA treatment presented less distinct, lacking structure and homogeneity, comparable to the observations after CCI (Fig. 5A). In the high resolution, we could demonstrate that both proteins were visibly co-localized in the perineurium (Fig. 5B). Qualitative observations were partly confirmed by semiquantitative analysis: Fluorescence intensity for ZO-1 decreased 2 h after rtPA injection (36.8 ± 22.1%, n = 3, p = 0.0454) while it did not change significantly for JAM-C (88.8 ± 24.4%, n = 3, p = 0.6701) *t*-test (Fig. 5C).

We have previously shown that a single perineurial application of rtPA functionally unseals the BNB for up to 5 d [47]. In contrast to CCI, single injection of rtPA did not elicit alterations of paw withdrawal threshold for up to one week, as tested by von Frey filaments (Fig. 6A). Moreover, histological screening for macrophage infiltration showed intact neural structures and no macrophage invasion after a single rtPA injection inducing barrier permeability for 5 d (Fig. 6B). This was in sharp contrast to a massive macrophage infiltration 1 week after CCI.

### 3.3. miR-155-5p upregulation both in CCI and after rtPA

Six hours after CCI, miR-155-5p was around 8-fold upregulated in the sciatic nerve compared to baseline expression and ~2-fold compared to sham. Such pattern was consistent for the entire observational period of 14 d (Fig. 7A). After rtPA injection, miR-155-5p was significantly increased, albeit to a much lesser degree, about 1.2-fold (Fig. 7B).

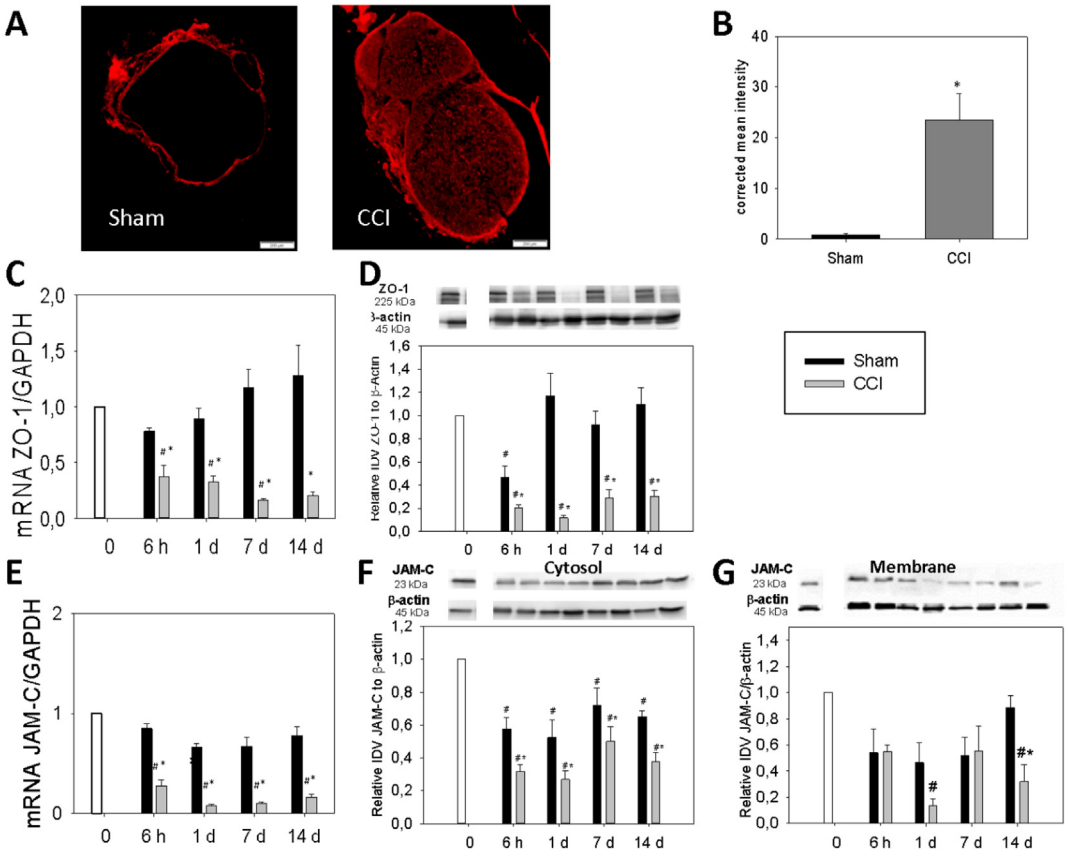


**Fig. 2.** BNB impairment and reduced tight junction protein and adherens junction protein expression after CCI. **A** One day after CCI surgery or sham operation, the sciatic nerve was harvested and permeability analyzed by ex vivo EBA immersion. n = 5, representative sample. Scale bar 200 µm. **B** Semi-quantification of endoneurial fluorescence intensity. * $p < 0.05$ (*t*-test). **C-G** At indicated time points after CCI surgery (grey) or sham operation (black), ZO-1 (**C, D**) and JAM-C (**E, F-G**) mRNA or protein were quantified. For mRNA quantification in sciatic nerves values from naïve mice were set at 1 (white). Original blots are displayed above the respective densitometric quantification (**D, F, G**). Protein expression of JAM-C was analyzed separately in the Triton X-100 soluble (**F**) and insoluble fraction (**G**), considered to contain "cytosolic" and "membrane" proteins, respectively. E ZO-1 was only quantified in the soluble fraction, in comparison to β-actin (45 kDa). # $p < 0.05$ compared to naïve animals, * $p < 0.0.5$ compared to sham-operated animals. n = 6, two-way ANOVA and Holm-Sidak post hoc test. All data are presented as mean ± SEM. IDV = integrated density value.

## 4. Discussion

In this study, we demonstrate that exogenous application of rtPA as well as ligation of the sciatic nerve in neuropathy result in a decrease of ZO-1 and JAM-C expression but with different kinetics, immunological responses, tissue damages and behavioral consequences. Moreover, local rtPA application and to a larger extend CCI lead to an upregulation of miR-155-5p.

### 4.1. tPA in neuropathy

In our study, we provide evidence that tPA is part of a pathway for barrier regulation. While tPA is widely known for its antithrombotic effect as plasmin generator, it is also relevant for barrier tightness: tPA expression on brain microvascular endothelial cells is strongly associated with BBB permeability [46]. This leaking effect is postulated to work via MMP-9 and -3 in brain endothelial cells, which both degrade tight junction proteins [28], such as claudin-5, occludin, and ZO-1. Moreover, knockdown of endogenous tPA reduces MMP-9 activity after middle cerebral artery occlusion [48]. The question whether tPA is beneficial or damaging after injury remains to be solved. Abe et al. have described a neuroprotective effect of tPA deficiency after spinal trauma [1]. In contrast, tPA application leads to enhanced functional recovery after neuronal trauma [53]. However, we do not regard those observations as contradictory: As outlined above, one key feature of tPA comprises fibrinolysis and decrease in collagen and myelin. Thus, a positive effect on functional recovery seems plausible as fibrin deposition, adhesions and scarring may be reduced. At the same time, these very mechanisms may impair features of the barrier homeostasis. Hence, both phenomena could be just two sides of one mechanism. In accordance with Yong et al. [49], we observed temporal upregulation of endogenous tPA after peripheral nerve injury. As tPA can be produced in Schwann cells [2], an effect on ZO-1 and JAM-C seems plausible. TPA binds to LRP-1 expressed on Schwann cells [11,24] and perineurial cells [54]. Binding of rtPA to LRP-1 can induce c-Jun phosphorylation suggesting that Schwann cell LRP-1 functions as an injury-detection receptor in the PNS [11]. Moreover, application of exogenous tPA enhances regeneration and functional recovery due to axon sprouting, clearance of myelin and fibrinogen as well as decrease in collagen scars [53].

### 4.2. Sequelae of rtPA-induced BNB opening

Compared to CCI-induced neuropathy with tPA upregulation, several differences need to be pointed out after a single perineural injection of rtPA. First, effects of rtPA have a quick onset: 2 h after application, transcriptional and mechanistic effects such as BNB opening can be seen. Downregulation of tight and adherens junction protein as well as upregulation of miR-155-5p are less pronounced compared to CCI. Moreover, the application is not accompanied with, and thus does not induce inflammatory or neuropathic features such as macrophage infiltration. This confirms results of earlier studies with rtPA [47]. While

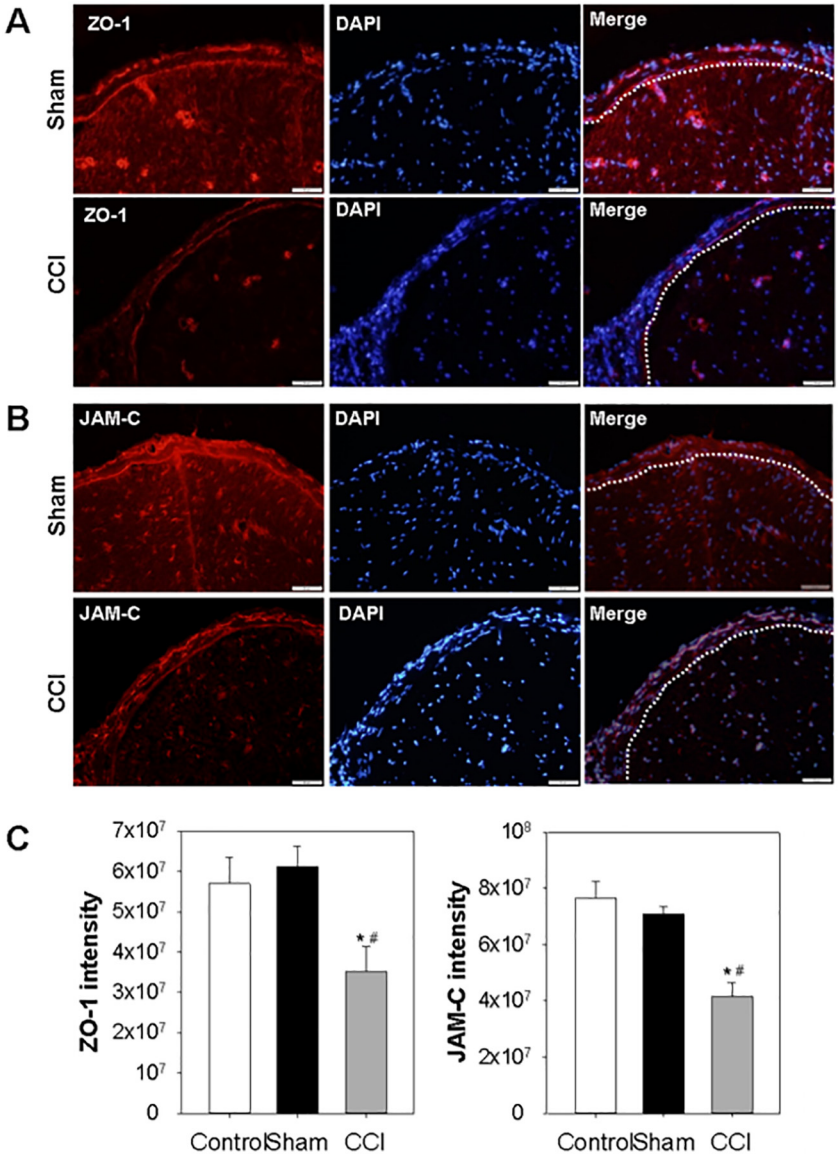


**Fig. 3.** Changes in immunoreactivity of JAM-C and ZO-1 after CCI. **A** Sections of the sciatic nerve 1 d after CCI were stained with a mouse monoclonal anti-ZO-1 Ab and compared to sham operation. Dotted lines mark the barrier between the perineurium (P) and endoneurium (E). **B** Similarly, staining with a rabbit polyclonal anti-JAM-C Ab was performed in CCI and sham rats and co-stained with DAPI. n = 6, representative samples. Scale bar 50 μm. **C** Semi-quantification of fluorescence intensity for ZO-1 and JAM-C in naïve control, sham-operated and CCI mice. n = 6, # $p < 0.05$ compared to naïve, * $p < 0.05$ compared to sham.ANOVA and Holm-Sidak post hoc test.

it could be shown in earlier work that rtPA modulates nociception by facilitating entry of pro- or analgesic drugs, it does not have an intrinsic modulatory effect. Therefore, we think that rtPA is also a suitable enhancer to deliver drugs to peripheral nerves e.g. in regional anesthesia.

### *4.3. ZO-1 and the ZO-1/JAM-C complex as a crucial player in BNB homoeostasis*

ZO-1 is a cytoplasmatic TJ-associated protein, organizing its composition by connecting tight junction proteins to the cortical actin cytoskeleton (reviewed in [12]). Moreover, it determines the polymerization status of claudins [40]. ZO-1 deficiency disrupts TJs, and reduced ZO-1 levels are associated with barrier breakdown in many neurological disorders [16]. We have previously shown that ZO-1 is robustly downregulated in the blood spinal cord barrier after CCI [35]. JAM-C is one of the adherens junction proteins linked to the cytoskeleton through ZO-1. While mainly described in leukocyte migration, it has been also studied in nerve injury: Avari et al. showed downregulation after sciatic crush injury, followed by recuperation in the further course, correlating with remyelination of the nerve [3]. Interestingly, JAM-C and ZO-1 were also transiently and slightly downregulated in sham animals. Apparently, the sham surgery alone with exposure of the sciatic nerve results in a minor trauma, possibly with a transient posttraumatic inflammatory reaction. This confirms the importance of comparison to a sham group to exclude confounding factors stemming from the surgery itself.

Whereas our and others' previous research was mainly focusing on other tight junction proteins such as claudins or occludin in the BNB [20,26], a functional complex of ZO-1 and the adherens junction protein JAM-C seems central for regular neuronal function: As it is highly expressed in Schwann cells, it not only shields the nerve from external influence but also contributes to proper neuronal conduction. This is confirmed by the phenotype of the JAM-C KO mice which exhibit a thick and loose myelin sheath and defect nerve conduction, leading to motor abnormalities such as decreased stride length and grip strength [37]. Moreover, its role in pain is underlined by transgenic studies: In a Schwann cell conditional KO model, hypersensitivity was observed [5]. In our study, we found JAM-C not only in Schwann cells but also in the perineurium, where immunoreactivity is significantly lowered in neuropathy but only as a trend after rtPA application. Furthermore, reduction in JAM-C protein is location-dependent on a subcellular level, with a decrease mainly in the cytoplasm: After both CCI and rtPA, the abundance of JAM-C in the “membrane protein” fraction recovers intermittently while JAM-C mRNA and “cytosol” protein are consistently

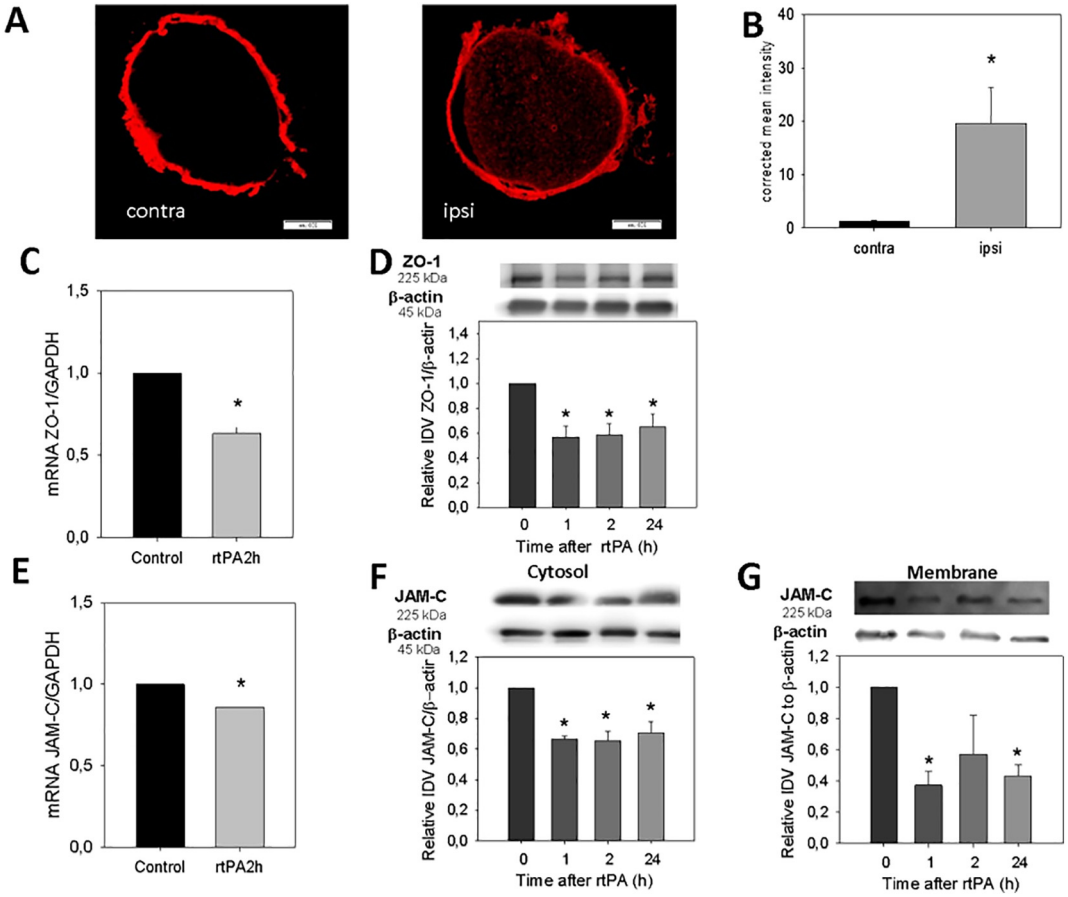


**Fig. 4.** BNB impairment and tight junction protein and adherens junction protein downregulation after a single perineural rtPA injection. **A** Wistar rats received a perisciatic injection of 10 μg rtPA, sciatic nerves were harvested after 2 h and immersed ex vivo in EBA and compared to the contralateral side. n = 5, representative sample. Scale bar 200 μm. **B** Semiquantification of endoneurial fluorescence intensity after rtPA. * $p < 0.05$,n = 5, *t*-test. **C, E** ZO-1 and JAM-C mRNA levels were measured in the sciatic nerve after 2 h. ZO-1 (**D**) and JAM-C (**F, G**) protein expression were analyzed 1–24 h after rtPA or solvent injection in relation to β-actin (45 kDa). JAM-C was quantified in the Triton 100-X soluble and insoluble ("cytosolic" and "membrane") fraction. Original representative blots are shown above the respective densitometric quantification. * $p < 0.05$ compared to solvent control. n = 8, one-way ANOVA, Holm-Sidak post-hoc test. All data are presented as mean ± SEM. IDV = integrated density value.

decreased. Interestingly, a more pronounced decrease of tight junction protein mRNA and proteins in the cytosol has also recently been described for several tight junction proteins such as claudin-1, claudin-19, and tricellulin in the blood spinal-cord barrier [35].

Two explanations for the discrepancy can be discussed, changes in protein degradation or intracellular shuffling: Altered conditions in CCI and rtPA might lead to a temporary reduction of protein degradation. However, given the intermediate recovery (at d 7 in CCI, and 2 h after rtPA, i.e. at full phenotype) in the membrane as opposed to cytosol, an intracellular translocation leading to a depletion in the cytoplasmatic pool is conceivable. This would explain the observed downregulation in mRNA as well as the discrepancy between both fractions. After initial downregulation (1 d after CCI, 1 h after rtPA), the membrane protein is partly recuperated through shift from the cytosol (7 d after CCI, 2 h after rtPA). However, such translocation cannot compensate for the reduction in the long run: Due to reduced transcription and translation, membrane protein is eventually reduced as well. Interestingly, however, barrier function was impaired at the time points of partial recovery in both models. Here, factors other than quantitative changes should be considered. It is known, for example, that phosphorylation of claudins or occludin regulate barrier permeability and pore functions, depending on the site of modification [7,17].

### *4.4. MiR-155-5p as a facilitator of BNB opening*

MiR-155-5p can act upon several genes relevant in the BNB. Most notably, it has been shown to directly target claudin-1 in several barriers, e.g. in the BBB [22,29,30]. Thus, miR-155-5p opens the barrier probably via downregulation of claudin-1. ZO-1 and JAM-C downregulation is shown in our study after both exogenous rtPA (cf. [47]) and CCI (cf. [26]). miR-155-5p is a major miR upregulated in macrophages in response to diverse proinflammatory stimuli in atherosclerosis or in arthritis [23]. It seems to sustain activity of LRP-1. Activation of LPR-1 via MMP9 results in downregulation of claudin-1 in the perineurium and barrier breakdown[13].In our study here, we showed a pronounced upregulation of miR-155-5p in the sciatic nerve after CCI and, albeit to lesser degree, after rtPA application. Interestingly, surgery itself as in sham animals seemed to mildly increase miR-155-5p expression. This is more pronounced after CCI, corresponding with hyperalgesia and macrophage infiltration. Therefore, miR-155-5p upregulation can be interpreted as a response to inflammatory stimuli like the ligature, possibly LPR-1-dependent. Several intracellular pathways are involved in barrier opening. For example, perineurial barrier opening and claudin-1 transcription are dependent on the ERK [47] and the wnt/catenin pathway [36]. Erk phosphorylation is increased after rtPA-induced barrier opening [47]. Barrier opening can be reversed by inhibitors of the glycogen-synthase kinase 3, possibly via an increase of catenin and the homeobox transcription factor cdx2, binding the

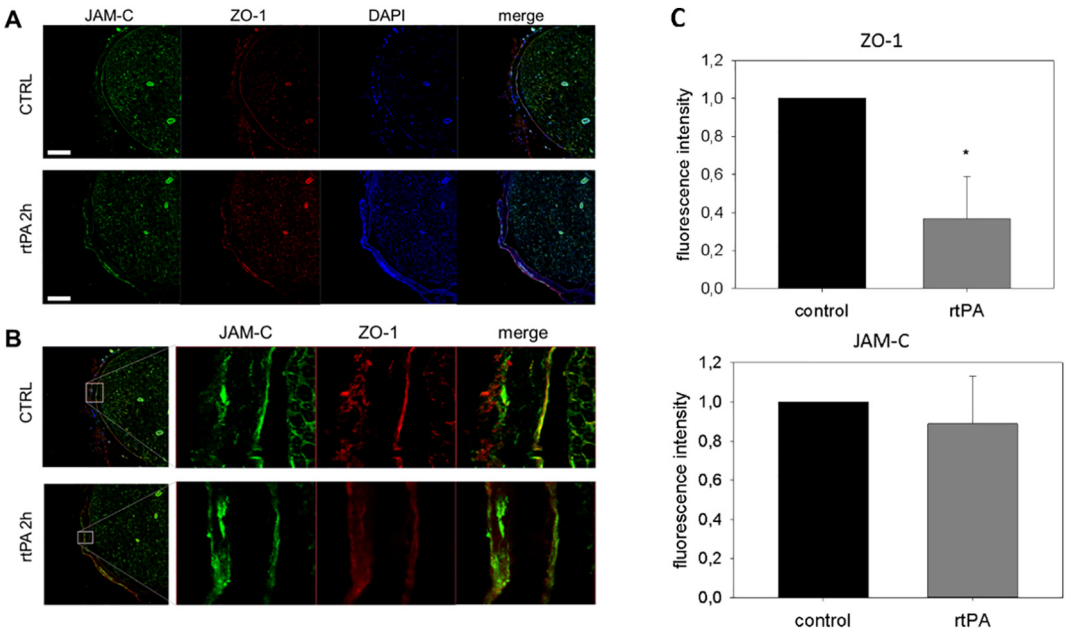


**Fig. 5.** Altered barrier structure and loss of ZO-1 and JAM-C immunoreactivity after perineural rtPA injection. Wistar rats were injected perineurally with 10 µg rtPA or solvent (control). **A** After 2 h the sciatic nerve was harvested and stained with a rabbit polyclonal anti-JAM-C Ab (green) and a mouse monoclonal anti-ZO-1 Ab (red). Scale bar 100 µm. **B** A further magnification enlarges the perineurium. Representative samples. Scale bar 20 µm. n = 3. **C** Semiquantification of fluorescence intensity for ZO-1 (top) and JAM-C (bottom). * $p < 0.05$, n = 3, *t*-test.

claudin-1 promoter [27,36,52]. This is in line with a study by Wu et al. They showed that miR-155 regulates the wnt/catenin pathway [44]. Much less is known about the influence of miR-155 on other tight junctions or adherens junction proteins. Further experiments are necessary to elucidate by which pathway miR-155 exerts an effect on the barrier. Interestingly, tPA is upregulated only several days after CCI while ZO-1 and JAM-C as well as miR-155-p show earlier alterations. In contrast, rtPA application induces changes in all three genes. This indicates a relationship more complex and multifaceted than mere one-way regulation between (r)tPA, miR-155-5p and tight junction proteins and adherens junction proteins. It has been shown that other miRs can regulate barrier function, e.g. miR-29b [51]and miR-183 [47]. Their role is often complex and depending on the context.

In summary, miR-155, LRP-1 activation, Erk phosphorylation and reduced wnt signaling via decreased catenin translocation open the BNB and downregulate tight and adherens junction proteins.

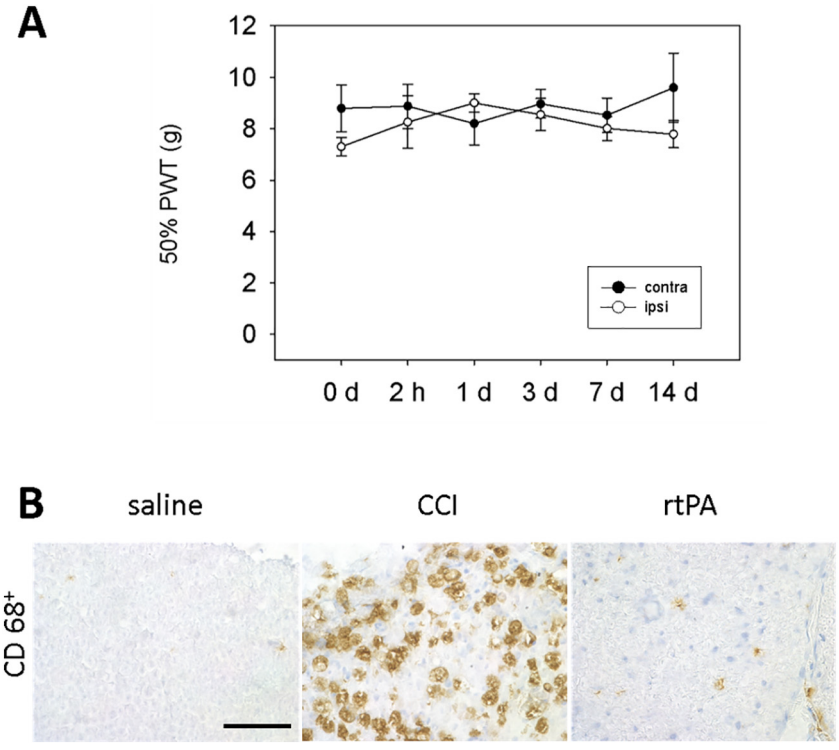


**Fig. 6.** No long-term mechanical hypersensitivity or macrophage infiltration after a single perisciatic rtPA application. **A** 10 µg rtPA was applied perineurally. Paw withdrawal thresholds were measured before and at indicated time points after rtPA application for up to 14 d and compared to the contralateral side. n = 5, $p > 0.05$ two-way RM ANOVA. Data presented as means ± SEM. **B** Seven days after rtPA application or after CCI, sections of the sciatic nerve were stained with a mouse monoclonal anti-CD68 antibody (representative samples. n = 3, scale bar 75 µm).

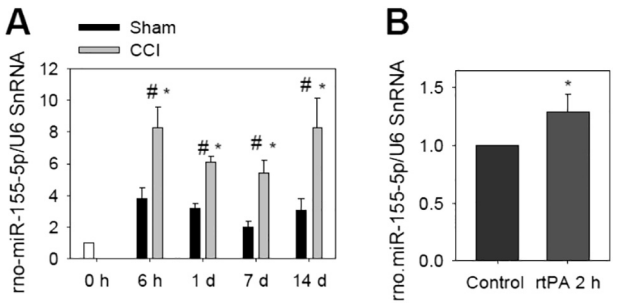


**Fig. 7.** miR-155-5p upregulation predominantly after CCI and to a lesser extend after perisciatic rtPA application. **A** After 6 h – 14 d CCI or after sham operation, miR-155-5p was quantified in the sciatic nerve. # $p < 0.05$ compared to baseline (untreated animals), * $p < 0.05$ compared to sham. n = 6, two-way ANOVA, Holm-Sidak post-hoc test. **B** Likewise, miR-155-5p levels in the sciatic nerve were determined 2 h after perisciatic rtPA injection compared to solvent injection. *$p < 0.05$. n = 8, *t*-test. All data are presented as mean ± SEM.

### 4.5. Limitations of the study

In this study, we used a common model, CCI, to study neuropathic pain. Other models like spared nerve injury, chemotherapy-induced or diabetic neuropathy might provide further insight whether barrier breakdown is a more general phenome in neuropathy or whether this is limited to this type of neuropathy which is characterized also by immune cell infiltration. The application of the 3R criteria (replacement, refinement and reduction) influence the study because the models chosen have a rather mild phenotype and not a large impact on quality of life of these animals [42].

## 5. Conclusions

In summary, we provide evidence that both exogenous rtPA and CCI with consequent tPA overexpression lead to breakdown of the BNB, including downregulation of the ZO-1/JAM-C complex. However, rtPA application has different kinetics and on its own does not lead to hyperalgesia. MiR-155-5p, known to regulate tight junction proteins, is increased mainly after CCI but also perineural rtPA application. Future studies could elucidate the therapeutic potential of miR-155-5p antagomirs or tPA blockers in neuropathic pain in patients or miR-155-5p could be used as a biomarker for neuropathic pain [19].

## Transparency document

The Transparency document associated with this article can be found, in online version.

## Acknowledgements

The Else-Kröner-Fresenius-Foundation, EKFS, 2014_A257 (HR), the Interdisciplinary Center of Clinical Research (IZKF) Würzburg, Z-2/61, (AKR), and funds from the university supported the study. The authors declare no conflict of interest. The research from the ncRNAPain project leading to these results has received funding from the European Union Seventh Framework Program (FP7/2007-2013) under grant agreement 602133 (HR).

We greatly thank Claudia Sommer, Katrin Doppler, Dept Neurology, University Hospital of Wuerzburg, as well as Benedikt Niedermirtl, Dept Anesthesiology, University Hospital of Wuerzburg, for help with the macrophage stains.

## References

[1] Y. Abe, H. Nakamura, O. Yoshino, T. Oya, T. Kimura, Decreased neural damage after spinal cord injury in tPA-deficient mice, J. Neurotrauma 20 (2003) 43–57.
[2] K. Akassoglou, K.W. Kombrinck, J.L. Degen, S. Strickland, Tissue plasminogen activator-mediated fibrinolysis protects against axonal degeneration and demyelination after sciatic nerve injury, J. Cell Biol. 149 (2000) 1157–1166.
[3] P. Avari, W. Huang, S. Averill, B. Colom, B.A. Imhof, S. Nourshargh, J.V. Priestley, The spatiotemporal localization of JAM-C following sciatic nerve crush in adult rats, Brain Behav. 2 (2012) 402–414.
[4] T. Berta, Y.C. Liu, Z.Z. Xu, R.R. Ji, Tissue plasminogen activator contributes to morphine tolerance and induces mechanical allodynia via astrocytic IL-1beta and ERK signaling in the spinal cord of mice, Neuroscience 247 (2013) 376–385.
[5] B. Colom, Y. Poitelon, W. Huang, A. Woodfin, S. Averill, U. Del Carro, D. Zambroni, S.D. Brain, M. Perretti, A. Ahluwalia, J.V. Priestley, T. Chavakis, B.A. Imhof, M.L. Feltri, S. Nourshargh, Schwann cell-specific JAM-C-deficient mice reveal novel expression and functions for JAM-C in peripheral nerves, FASEB J. 26 (2012) 1064–1076.
[6] W.J. Dixon, F.J. Massey, Sensitivity experiments. Introduction to Statistical Analysis, McGraw Hill, 1969, pp. 377–394.
[7] M.J. Dörfel, O. Huber, Modulation of tight junction structure and function by kinases and phosphatases targeting occludin, J Biomed Biotechnol 2012 (2012) 807356.
[8] K. Ebnet, A. Suzuki, S. Ohno, D. Vestweber, Junctional adhesion molecules (JAMs): more molecules with dual functions? J. Cell Sci. 117 (2004) 19–29.
[9] F. Faul, E. Erdfelder, A. Buchner, A.G. Lang, Statistical power analyses using G*power 3.1: tests for correlation and regression analyses, Behav. Res. Methods 41 (2009) 1149–1160.
[10] N.B. Finnerup, N. Attal, S. Haroutounian, E. McNicol, R. Baron, R.H. Dworkin, I. Gilron, M. Haanpaa, P. Hansson, T.S. Jensen, P.R. Kamerman, K. Lund, A. Moore, S.N. Raja, A.S. Rice, M. Rowbotham, E. Sena, P. Siddall, B.H. Smith, M. Wallace, Pharmacotherapy for neuropathic pain in adults: a systematic review and meta-analysis, Lancet Neurol. 14 (2015) 162–173.
[11] A. Flutsch, K. Henry, E. Mantuano, M.S. Lam, M. Shibayama, K. Takahashi, S.L. Gonias, W.M. Campana, Evidence that LDL receptor-related protein 1 acts as an early injury detection receptor and activates c-Jun in Schwann cells, Neuroreport 27 (2016) 1305–1311.
[12] D. Günzel, A.S. Yu, Claudins and the modulation of tight junction permeability, Physiol. Rev. 93 (2013) 525–569.
[13] D. Hackel, A. Brack, M. Fromm, H.L. Rittner, Modulation of tight junction proteins in the perineurium for regional pain control, Ann. N. Y. Acad. Sci. 1257 (2012) 199–206.
[14] IASP, I.A.f.t.S.o.P., IASP Guidelines for the Use of Animals in Research. Retrieved on Jan 08, 2019 (https://www.iasp-pain.org/Education/Content.aspx?ItemNumber=1217)
[15] M. Itoh, H. Sasaki, M. Furuse, H. Ozaki, T. Kita, S. Tsukita, Junctional adhesion molecule (JAM) binds to PAR-3: a possible mechanism for the recruitment of PAR-3 to tight junctions, J. Cell Biol. 154 (2001) 491–497.
[16] T. Katsuno, K. Umeda, T. Matsui, M. Hata, A. Tamura, M. Itoh, K. Takeuchi, T. Fujimori, Y. Nabeshima, T. Noda, S. Tsukita, Deficiency of zonula occludens-1 causes embryonic lethal phenotype associated with defected yolk sac angiogenesis and apoptosis of embryonic cells, Mol. Biol. Cell 19 (2008) 2465–2475.
[17] G. Krause, L. Winkler, S.L. Mueller, R.F. Haseloff, J. Piontek, I.E. Blasig, Structure and function of claudins, Biochim. Biophys. Acta 1778 (2008) 631–645.
[18] D. Labuz, Y. Schmidt, A. Schreiter, H.L. Rittner, S.A. Mousa, H. Machelska, Immune cell-derived opioids protect against neuropathic pain in mice, J. Clin. Invest. 119 (2009) 278–286.
[19] M. Leinders, N. Uceyler, A. Thomann, C. Sommer, Aberrant microRNA expression in patients with painful peripheral neuropathies, J. Neurol. Sci. 380 (2017) 242–249.
[20] T.K. Lim, X.Q. Shi, H.C. Martin, H. Huang, G. Luheshi, S. Rivest, J. Zhang, Blood-nerve barrier dysfunction contributes to the generation of neuropathic pain and allows targeting of injured nerves for pain relief, Pain 155 (5) (2014) 5954–5967.
[21] K.J. Livak, T.D. Schmittgen, Analysis of relative gene expression data using real-time quantitative PCR and the 2(−Delta Delta C(T)) method, Methods 25 (2001) 402–408.
[22] M.A. Lopez-Ramirez, D. Wu, G. Pryce, J.E. Simpson, A. Reijerkerk, J. King-Robson, O. Kay, H.E. de Vries, M.C. Hirst, B. Sharrack, D. Baker, D.K. Male, G.J. Michael, I.A. Romero, MicroRNA-155 negatively affects blood-brain barrier function during neuroinflammation, FASEB J. 28 (2014) 2551–2565.
[23] E. Mantuano, C. Brifault, M.S. Lam, P. Azmoon, A.S. Gilder, S.L. Gonias, LDL receptor-related protein-1 regulates NFkappaB and microRNA-155 in macrophages to control the inflammatory response, Proc. Natl. Acad. Sci. U. S. A. 113 (2016) 1369–1374.
[24] E. Mantuano, G. Inoue, X. Li, K. Takahashi, A. Gaultier, S.L. Gonias, W.M. Campana, The hemopexin domain of matrix metalloproteinase-9 activates cell signaling and promotes migration of schwann cells by binding to low-density lipoprotein receptor-related protein, J. Neurosci. 28 (2008) 11571–11582.
[25] K. Mishiro, M. Ishiguro, Y. Suzuki, K. Tsuruma, M. Shimazawa, H. Hara, A broad-spectrum matrix metalloproteinase inhibitor prevents hemorrhagic complications induced by tissue plasminogen activator in mice, Neuroscience 205 (2012) 39–48.
[26] N. Moreau, A. Mauborgne, S. Bourgoin, P.O. Couraud, I.A. Romero, B.B. Weksler, L. Villanueva, M. Pohl, Y. Boucher, Early alterations of hedgehog signaling pathway in vascular endothelial cells after peripheral nerve injury elicit blood-nerve barrier disruption, nerve inflammation, and neuropathic pain development, Pain 157 (2016) 827–839.
[27] N. Moreau, A. Mauborgne, P.O. Couraud, I.A. Romero, B.B. Weksler, L. Villanueva, M. Pohl, Y. Boucher, Could an endoneurial endothelial crosstalk between Wnt/beta-catenin and sonic hedgehog pathways underlie the early disruption of the infra-orbital blood-nerve barrier following chronic constriction injury? Mol. Pain 13 (2017) 1744806917727625.

[28] B. Niego, R.L. Medcalf, Plasmin-dependent modulation of the blood-brain barrier: a major consideration during tPA-induced thrombolysis? J. Cereb. Blood Flow Metab. 34 (2014) 1283–1296.
[29] J.C. Pena-Philippides, A.S. Gardiner, E. Caballero-Garrido, R. Pan, Y. Zhu, T. Roitbak, Inhibition of MicroRNA-155 supports endothelial tight junction integrity following oxygen-glucose deprivation, J. Am. Heart Assoc. 7 (2018).
[30] W. Qin, Q. Ren, T. Liu, Y. Huang, J. Wang, MicroRNA-155 is a novel suppressor of ovarian cancer-initiating cells that targets CLDN1, FEBS Lett. 587 (2013) 1434–1439.
[31] A. Reijerkerk, M.A. Lopez-Ramirez, B. van Het Hof, J.A. Drexhage, W.W. Kamphuis, G. Kooij, J.B. Vos, T.C. van der Pouw Kraan, A.J. van Zonneveld, A.J. Horrevoets, A. Prat, I.A. Romero, H.E. de Vries, MicroRNAs regulate human brain endothelial cell-barrier function in inflammation: implications for multiple sclerosis, J. Neurosci. 33 (2013) 6857–6863.
[32] A.K. Reinhold, H.L. Rittner, Barrier function in the peripheral and central nervous system-a review, Pflugers Arch. 469 (2017) 123–134.
[33] A.K. Reinhold, J. Schwabe, T.J. Lux, E. Salvador, H.L. Rittner, Quantitative and structural changes of the blood-nerve barrier in peripheral neuropathy, Front. Neurosci. 12 (2018) 936, , https://doi.org/10.3389/fnins.2018.00936.
[34] I. Sagot, F. Regnouf, J.P. Henry, L.A. Pradel, Translocation of cytosolic annexin 2 to a triton-insoluble membrane subdomain upon nicotine stimulation of chromaffin cultured cells, FEBS Lett. 410 (1997) 229–234.
[35] R.S. Sauer, J. Kirchner, S. Yang, L. Hu, M. Leinders, C. Sommer, A. Brack, H.L. Rittner, Blood-spinal cord barrier breakdown and pericyte deficiency in peripheral neuropathy, Ann. N. Y. Acad. Sci. 1405 (2017) 71–88.
[36] R.S. Sauer, S.M. Krug, D. Hackel, C. Staat, N. Konasin, S. Yang, B. Niedermirtl, J. Bosten, R. Gunther, S. Dabrowski, K. Doppler, C. Sommer, I.E. Blasig, A. Brack, H.L. Rittner, Safety, efficacy, and molecular mechanism of claudin-1-specific peptides to enhance blood-nerve-barrier permeability, J. Control. Release 185 (2014) 88–98.
[37] C. Scheiermann, P. Meda, M. Aurrand-Lions, R. Madani, Y. Yiangou, P. Coffey, T.E. Salt, D. Ducrest-Gay, D. Caille, O. Howell, R. Reynolds, A. Lobrinus, R.H. Adams, A.S. Yu, P. Anand, B.A. Imhof, S. Nourshargh, Expression and function of junctional adhesion molecule-C in myelinated peripheral nerves, Science 318 (2007) 1472–1475.
[38] C. Sommer, J.A. Galbraith, H.M. Heckman, R.R. Myers, Pathology of experimental compression neuropathy producing hyperesthesia, J. Neuropathol. Exp. Neurol. 52 (1993) 223–233.
[39] C. Sommer, A. Lalonde, H.M. Heckman, M. Rodriguez, R.R. Myers, Quantitative neuropathology of a focal nerve injury causing hyperalgesia, J. Neuropathol. Exp. Neurol. 54 (1995) 635–643.
[40] K. Umeda, J. Ikenouchi, S. Katahira-Tayama, K. Furuse, H. Sasaki, M. Nakayama, T. Matsui, S. Tsukita, M. Furuse, ZO-1 and ZO-2 independently determine where claudins are polymerized in tight-junction strand formation, Cell 126 (2006) 741–754.
[41] I. Uno, T. Ueda, P. Greenglad, Differences in properties of cytosol and membrane-derived protein kinases, J. Biol. Chem. 251 (1976) 2192–2195.
[42] R. Urban, G. Scherrer, E.H. Goulding, L.H. Tecott, A.I. Basbaum, Behavioral indices of ongoing pain are largely unchanged in male mice with tissue or nerve injury-induced mechanical hypersensitivity, Pain 152 (2011) 990–1000.
[43] O. van Hecke, S.K. Austin, R.A. Khan, B.H. Smith, N. Torrance, Neuropathic pain in the general population: a systematic review of epidemiological studies, Pain 155 (2014) 654–662.
[44] X. Wu, Y. Wang, T. Yu, E. Nie, Q. Hu, W. Wu, T. Zhi, K. Jiang, X. Wang, X. Lu, H. Li, N. Liu, J. Zhang, Y. You, Blocking MIR155HG/miR-155 axis inhibits mesenchymal transition in glioma, Neuro-Oncology 19 (2017) 1195–1205.
[45] H. Yamanaka, K. Obata, T. Fukuoka, Y. Dai, K. Kobayashi, A. Tokunaga, K. Noguchi, Tissue plasminogen activator in primary afferents induces dorsal horn excitability and pain response after peripheral nerve injury, Eur. J. Neurosci. 19 (2004) 93–102.
[46] F. Yang, S. Liu, S.J. Wang, C. Yu, A. Paganini-Hill, M.J. Fisher, Tissue plasminogen activator expression and barrier properties of human brain microvascular endothelial cells, Cell. Physiol. Biochem. 28 (2011) 631–638.
[47] S. Yang, S.M. Krug, J. Heitmann, L. Hu, A.K. Reinhold, S. Sauer, J. Bosten, C. Sommer, M. Fromm, A. Brack, H.L. Rittner, Analgesic drug delivery via recombinant tissue plasminogen activator and microRNA-183-triggered opening of the blood-nerve barrier, Biomaterials 82 (2016) 20–33.
[48] M. Yepes, M. Sandkvist, E.G. Moore, T.H. Bugge, D.K. Strickland, D.A. Lawrence, Tissue-type plasminogen activator induces opening of the blood-brain barrier via the LDL receptor-related protein, J. Clin. Invest. 112 (2003) 1533–1540.
[49] N. Yong, C. Guoping, The role and mechanism of the up-regulation of fibrinolytic activity in painful peripheral nerve injury, Neurochem. Res. 34 (2009) 587–592.
[50] B. Zheng, W.N. Yin, T. Suzuki, X.H. Zhang, Y. Zhang, L.L. Song, L.S. Jin, H. Zhan, H. Zhang, J.S. Li, J.K. Wen, Exosome-mediated miR-155 transfer from smooth muscle cells to endothelial cells induces endothelial injury and promotes atherosclerosis, Mol. Ther. 25 (2017) 1279–1294.
[51] Q. Zhou, S. Costinean, C.M. Croce, A.R. Brasier, S. Merwat, S.A. Larson, S. Basra, G.N. Verne, MicroRNA 29 targets nuclear factor-kappaB-repressing factor and Claudin 1 to increase intestinal permeability, Gastroenterology 148 (158–169) (2015) e158.
[52] Y. Zhou, Y. Wang, M. Tischfield, J. Williams, P.M. Smallwood, A. Rattner, M.M. Taketo, J. Nathans, Canonical WNT signaling components in vascular development and barrier formation, J. Clin. Invest. 124 (2014) 3825–3846.
[53] T. Zou, C. Ling, Y. Xiao, X. Tao, D. Ma, Z.L. Chen, S. Strickland, H. Song, Exogenous tissue plasminogen activator enhances peripheral nerve regeneration and functional recovery after injury in mice, J. Neuropathol. Exp. Neurol. 65 (2006) 78–86.
[54] D. Zwanziger, D. Hackel, C. Staat, A. Bocker, A. Brack, M. Beyermann, H. Rittner, I.E. Blasig, A peptidomimetic tight junction modulator to improve regional analgesia, Mol. Pharm. 9 (2012) 1785–1794.